

ULTRAIINTENSE AND ULTRASHORT LASER PULSES FROM RAMAN AMPLIFICATION IN PLASMA FOR LASER-PLASMA ACCELERATORS*

Min Sup Hur[†], Hyyong Suk, Guang-Hoon Kim, KERI, Changwon, Korea
 Ryan Lindberg, Andy Charman, Jonathan Wurtele, LBNL, Berkeley, CA 94720, USA

Abstract

We present analysis and simulations of electron trapping effect in the Raman pulse amplification in plasma. An ultraintense and ultrashort laser pulse is a very essential part in an advanced acceleration scheme using laser and plasma. Recently many prominent experimental observations and simulations were reported, where laser pulses of a few terawatt in power and less than 100 fs in the duration were used. To make such strong pulses, a novel scheme of using Raman backscatter in plasma was proposed and has been studied intensively. The Raman amplification in plasma does not have a restriction in material damage threshold. However, for the new amplifier to be a promising alternative of the CPA technique, more extensive studies on various issues are required. One of the fundamental issues is the electron kinetic effect such as particle trapping or wavebreaking. We describe averaged-particle-in-cell (aPIC) scheme to simulate the Raman amplification system and discuss the particle trapping effect using the aPIC model.

INTRODUCTION

The novel scheme of using the Raman backscatter (RBS) in plasmas to amplify laser pulses (Fig. 1) is attracting the interests of many people in the laser-plasma community [1, 2, 3, 4, 5]. Since the plasma is free from the mater-

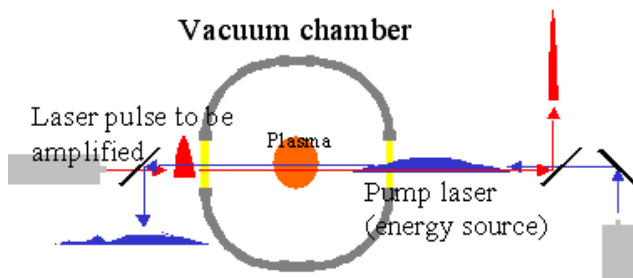


Figure 1: Schematics of the Raman backward amplifier.

ial damage, which is a very strong restriction in increasing the output power by the conventional chirped-pulse-amplification (CPA) technique, the new scheme is expected to be a promising alternative for obtaining ultra-powerful peta-watt laser pulses. Issues in the system are the kinetic effects [6] like Landau damping, ionization, wavebreaking, electron trapping, noise problem, and multi-

dimensional effects like diffraction, conservation of the focusing phase. We introduce first a newly developed modeling for the RBS simulation: the averaged-particle-in-cell (aPIC) method [5], which is an FEL-like envelope-particle model. Benchmark and the simulation of particle trapping effects are provided. A preliminary result of semi two dimensional aPIC simulation is also presented. We discuss on the physical meaning of the particle trapping.

APIC MODEL

In the concept of aPIC, the fast oscillation time scale of the lasers are averaged out, and the simulation time step resolves only the slowly varying laser envelopes and plasma motion. The larger time step in aPIC simulations enables much faster calculation than the general full particle-in-cell (PIC) method, while the averaged scheme includes every important plasma kinetic effects as in a full PIC.

Basic Equations

The basic equations of the aPIC model are the envelope equations of seed and pump lasers, the averaged equation of motion for simulation particles, and the Poisson equation to calculate the electrostatic longitudinal force. The driving current of lasers are obtained from averaging of ponderomotive phase of the simulation particles. The detailed derivation of the envelope equations of seed and pump lasers are described in Ref. [5].

The envelope equations of lasers are

$$\frac{\partial a_1}{\partial t} + c \frac{\partial a_1}{\partial z} = -i \frac{\omega_p^2}{2\omega_1} a_2 \left\langle \frac{e^{i\phi_j}}{\gamma_j} \right\rangle, \quad (1)$$

and

$$\frac{\partial a_2}{\partial t} - c \frac{\partial a_2}{\partial z} = -i \frac{\omega_p^2}{2\omega_2} a_1 \left\langle \frac{e^{-i\phi_j}}{\gamma_j} \right\rangle, \quad (2)$$

where we used $\omega_{1,2} \simeq ck_{1,2}$, valid for $\omega_p \ll \omega_{1,2}$. This is generally a good approximation for the regimes of interest in Raman amplification.

The equation of motion is

$$\frac{d\vec{p}_s}{dt} = -\frac{e}{mc} \vec{E}_s - \frac{c}{2\gamma} \nabla \left(\Re e[\vec{a}_1^* \cdot \vec{a}_2 e^{i\phi_{\text{PM}}}] \right), \quad (3)$$

where \vec{p}_s is the slowly varying part of the canonical momentum, which equals the longitudinal momentum ($\gamma v_z/c$). The uncoupled ponderomotive driving terms, which are respectively proportional to the derivative of the seed and pump intensity, are very small compared to the coupled term. Note that in Eq. (3), the ponderomotive

* Work supported by Creative Research Initiatives, Korea

[†] mshur@keri.re.kr

force only by the coupling (i.e., beat) of two laser pulses is included.

Benchmark

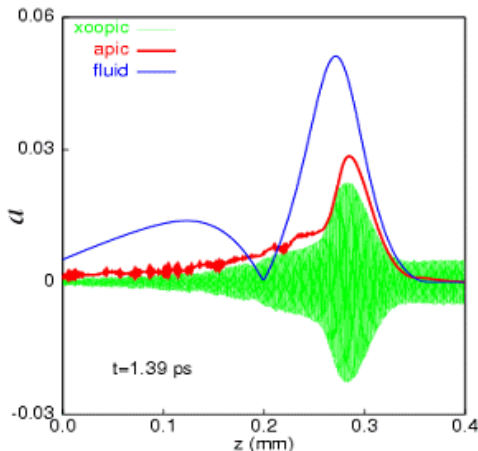


Figure 2: Comparison of Xoopic, aPIC, and fluid models.

The equations in the previous section were implemented in a one-dimensional (1D) simulation code. The 1D aPIC result was compared to the 1D full PIC code XOOPIE [7]. Figure 2 is a snapshot of the seed laser profile after 1.4 ps propagation through a plasma. Computation speed of the fluid code is fastest (calculation time less than 5 minutes). However, the deviation is big from other results from kinetic models. The XOOPIE and aPIC yielded almost same results. In case of the full PIC calculation (XOOPIE), the computation time was about 12 hours, while it was only 40 minutes in the aPIC simulation.

PARTICLE TRAPPING EFFECT

It is found from Fig. 2 that the fluid result deviates far from the kinetic results. This can be attributed to the absence of kinetic effects in the fluid model. Figure 3 shows electron trapping near the peak of the seed laser, captured from the aPIC simulation. As the trapped electrons are accelerated in the plasma-wave potential, the plasma wave loses energy to compensate it, and undergoes a frequency downshift. (In quantum mechanical language, this is just a consequence of the Planck-Einstein relations, as the energy transfer to trapped particles occurs less by conversion or absorption of plasmons than by the adiabatic red-shift of each plasmon's frequency.) Initially the system begins with resonance between the three waves, i.e. the frequency difference of the two lasers is tuned to match the plasma frequency. The growth rate of the Raman backscatter instability reaches the maximum when the resonance condition is satisfied. As amplification proceeds, the amplitude of the plasma wave increases until wave-breaking occurs. Then particles begin to be trapped in the plasma wave troughs, which leads to the breaking of the resonance due to the

frequency downshift of the plasma wave. The suppression or saturation of the Raman amplification is the very natural result of the dynamically induced resonance breaking. In Ref. [6], we derived a kinetic term and added it to the plasma equation of the three-wave model. The physical role of the kinetic term in the saturation of the Raman backscatter was successfully explained in the framework of the three-wave model. Mathematically rigorous description of this phenomena will be published soon [6].

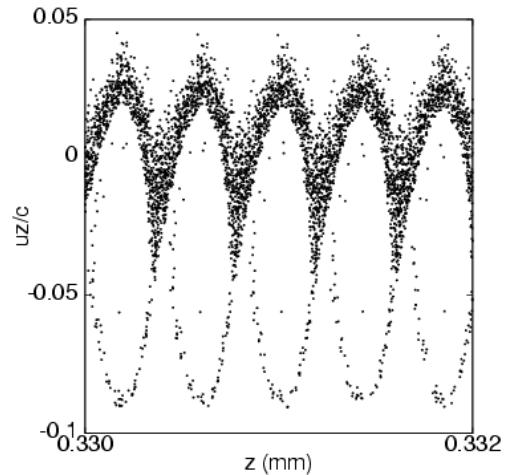


Figure 3: Particle trapping near the peak of the seed laser.

SEMI TWO-DIMENSIONAL SIMULATION

The extension of the aPIC code to multi-dimensions is under progress. One of the most important multi-dimensional effects is the preservation of the focusing phase of the seed. Typically the seed pulse is arranged so that it focuses onto some target and the amplification process is performed much before the focusing. Therefore it is required that the relative phase of the seed in the transverse direction be conserved during the Raman amplification. A preliminary simulation of a two dimensional cylindrically symmetric system is presented in Fig. 4. In the semi two-dimensional (2D) model, we assumed the transverse motion of the electrons is negligible. This is quite a reasonable assumption, since the longitudinal ponderomotive force by the two counter-propagating lasers is dominant. The transverse coupling occurs through the diffraction terms in the laser envelope equations. The figures in the left column in Fig. 4 represent the seed envelope at $t = 0$ and $t = 1.2$ ps. The transverse spot size of the seed decreased, which implies that the focusing phase of the seed was well preserved. However, more intense and systematic parameter scanning in various regimes is required to understand the relative phase change. The figures in the right column show the pump depletion.

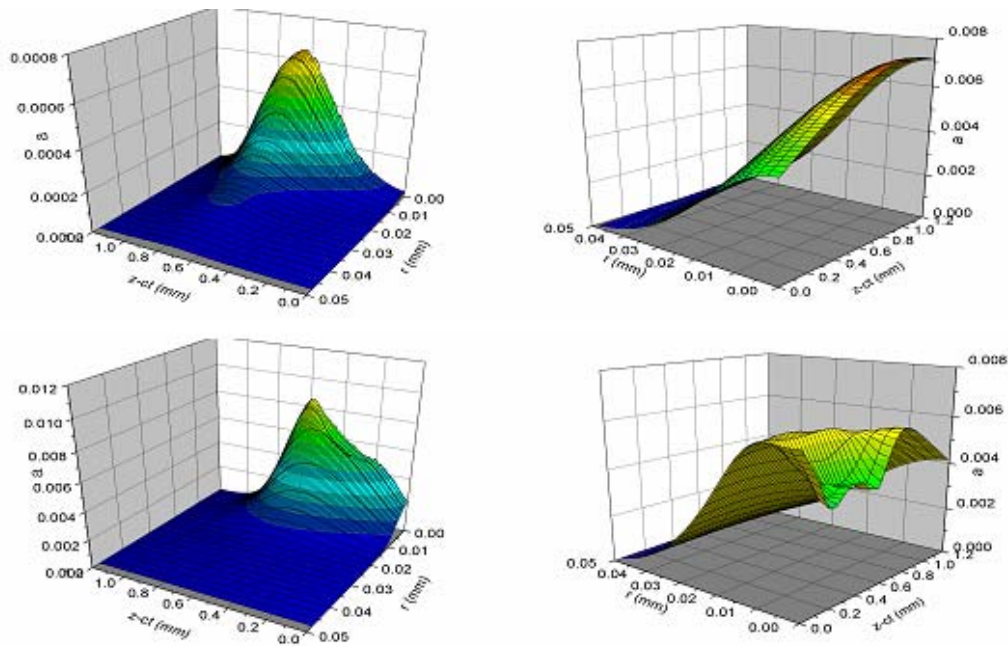


Figure 4: Semi two dimensional aPIC simulation.

CONCLUSION

The basic equations of aPIC model were described. The benchmark of the aPIC simulation against the full PIC code XOOPIC is excellent, while the computation speed is much larger in the aPIC. We discussed the electron kinetic effects. A preliminary semi-2D aPIC simulation was presented. This work was supported by the Creative Research Initiatives, Korea.

REFERENCES

- [1] V.M. Malkin, G. Shvets, and N.J. Fisch, *Physical Review Letters* 82 (1999) 4448.
- [2] V.M. Malkin, G. Shvets, and N.J. Fisch, *Physical Review Letters* 84 (2000) 1208.
- [3] D.S. Clark and N.J. Fisch, *Physics of Plasmas* 10 (2003) 3363.
- [4] W. Cheng, Y. Avitzour, Y. Ping, S. Suckewer, N.J. Fisch, M.S. Hur, and J.S. Wurtele, *Physical Review Letters* 94 (2005) 045003.
- [5] M.S. Hur, G. Penn, J.S. Wurtele, and R. Lindberg, *Physics of Plasmas* 11 (2004) 5204.
- [6] M.S. Hur, R. Lindberg, A. Charman, J. Wurtele, and H.Suk (submitted).
- [7] H. Usui, J.P. Verboncoeur, C.K. Birdsall, *IEICE Trans. Electronics* E83C (2000) 989.